AIAA JOURNAL
Vol. 32, No. 6, June 1994

Technical Notes

TECHNICAL NOTES are short manuscripts describing new developments or important results of a preliminary nature. These Notes cannot exceed 6 manuscript pages and 3 figures; a page of text may be substituted for a figure and vice versa. After informal review by the editors, they may be published within a few months of the date of receipt. Style requirements are the same as for regular contributions (see inside back cover).

Chemical Recombination in an Expansion Tube

Robert J. Bakos* and Richard G. Morgan†
University of Queensland,
Brisbane, Queensland 4072, Australia

Introduction

HYPERSONIC propulsion and aerothermal testing requirements continue to drive the development of ground facilities capable of duplicating energy, Reynolds number, and stream chemistry at near-orbital velocities. Expansion tube pulse facilities offer this capability if the theoretical operating cycle proposed by Trimpi[1] is accepted as representing the actual flow history. As shown in the distance-time (x-t) diagram (Fig. 1a), this requires that the secondary diaphragm rupture instantaneously on impact by the primary shock, and that its mass contributes no inertia to the test gas for subsequent acceleration. However, experiments by Shinn and Miller[2] with helium test gas have shown that for even the thinnest practical diaphragm (3.18 μm polyester film in a 152-mm-diam tube) the primary shock reflection off the diaphragm maintains sufficient strength to travel more than 110 mm upstream into the oncoming test gas. Because the test gas in an expansion tube originates from the vicinity of the diaphragm, it is processed by the reflected shock. For air test gas, the entropy generated may be sufficient to cause significant oxygen dissociation that can only be eliminated by recombination in the subsequent unsteady expansion. In this sense, the problem is similar to the nozzle freezing problem occurring in high-enthalpy reflected shock tunnels.

The details of the secondary diaphragm rupture will affect both the strength of the reflected shock generated and the rate of expansion experienced by the test gas as it accelerates under the influence of the unsteady expansion. This Note adopts a diaphragm inertia rupture model[3] assuming that the diaphragm shears cleanly around its periphery, remains intact and nearly planer, and provides no resistance other than its inertia to acceleration by the pressure field. The diaphragm acceleration relieves the pressure behind the reflected shock so that it weakens with time (Fig. 1b), lowering the test gas entropy and initial dissociation levels. Also, and perhaps more importantly, the diaphragm inertia limits the initial expansion rate, allowing effective recombination to be achieved.

For this situation an approximate analytical solution for the Lagrangian pressure-time history is presented for an ideal gas. A one-dimensional numerical solution with equilibrium chemistry for the diaphragm-inertia model was also done and shows good agreement with both the approximate analytical solution and a pressure measurement for air test gas from the NASA Langley HYPULSE expansion tube.[4] The extent of recombination is then calculated using a finite rate chemistry package for the analytically or numerically determined pressure-time history.

Calculations including the diaphragm inertia show significantly lower dissociation levels than those reported recently by Wilson[5] where the diaphragm was taken to hold fast for a specified holding time and then allowed to open instantaneously without contributing inertia to the subsequent acceleration (Fig. 1c). In Ref. 5, this model was used in a full one-dimensional, unsteady-flow calculation with finite rate chemistry. An approximate calculation of recombination for this rupture model is included here for comparison with the inertia model.

Finally, a two-parameter correlation summarizes the results of the nonequilibrium calculations for air in terms of the

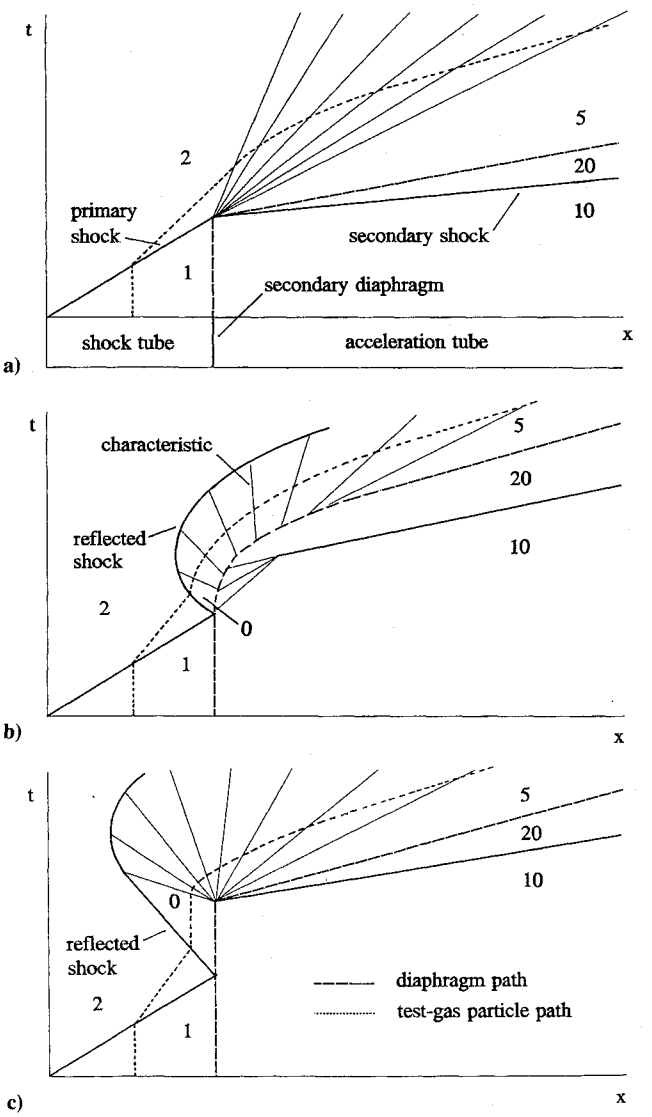

Fig. 1 x-t diagrams for secondary diaphragm rupture models: a) ideal diaphragm, b) inertial diaphragm and c) holding time diaphragm.

Received June 5, 1993; revision received Dec. 29, 1993; accepted for publication Jan. 3, 1994.

*Graduate Research Student, Department of Mechanical Engineering; currently Principal Scientist, General Applied Science Laboratories, 77 Raynor Avenue, Ronkonkoma, NY 11779. Member AIAA.

†Senior Lecturer, Department of Mechanical Engineering. Member AIAA.

postreflected shock thermodynamic properties and an inertial time scale for the diaphragm. This allows rapid estimation of nonequilibrium air compositions for any choice of diaphragm and suborbital test conditions in an expansion tube.

Analysis

Under the assumption of a peripheral diaphragm rupture, the diaphragm motion will proceed subject to its inertia and the pressure applied to either side. Therefore, the diaphragm acts as a very light piston separating the test and acceleration gases. Because typical prerun diaphragm pressure ratios are of the order 100–1000:1, pressure in the compressing acceleration gas is negligible (for the initial portion of the diaphragm motion) relative to the test gas pressure p_d, behind the reflected shock. The equation of motion for the diaphragm is

$$\frac{du}{dt} = \frac{p_d}{\rho_d w_d} \tag{1}$$

where ρ_d is the diaphragm density and w_d the thickness.

Following Meyer,[6] the gas between the diaphragm and the reflected shock is assumed to have a uniform value of the Riemann invariant $J_+ = 2a/(\gamma - 1) + u$, where a is the sound speed and u the gas motion velocity, such that the J_- characteristics will be straight lines emanating from the diaphragm surface. That is, the expansion occurs through a simple wave. Uniformity of J_+ requires that either the reflected shock be weak such that entropy changes across it can be ignored, or that it does not decay so that again a uniform entropy region exists behind it. For conditions of interest the initial reflected shock Mach number relative to the test gas is within the range $M_{rs} = 2$–3, which, although not weak, does not significantly alter the value of J_+. J_+ is evaluated behind the fully reflected shock and assumed not to vary; thus the diaphragm motion is equivalent to that caused by an infinite-length reservoir at the postreflected shock pressure and sound speed. This leads to the following relation for the pressure on the upstream face of the diaphragm,

$$\frac{p_d}{p_0} = \left(\frac{J_+ - u_d}{J_+}\right)^{2\gamma/\gamma - 1} \tag{2}$$

where subscript 0 refers to conditions behind the fully reflected shock. Introducing a velocity scale $u_R = 2a_0/(\gamma - 1)$ and an inertial time scale $t_R = 2\rho_d w_d a_0/(\gamma + 1)p_0$ for the diaphragm motion, integration of Eq. (1) with Eq. (2) gives for the diaphragm velocity

$$\frac{u_d}{u_R} = 1 - \left(1 + \frac{t}{t_R}\right)^{-(\gamma - 1)/(\gamma + 1)} \tag{3}$$

and for the pressure history of a particle adjacent to the diaphragm face,

$$\frac{p_d}{p_0} = \left(1 + \frac{t}{t_R}\right)^{-2\gamma/(\gamma + 1)} \tag{4}$$

The initial expansion rate at $t = 0$ is $dp_d/dt = -\gamma p_0^2/\rho_d \tau_d a_0$, which is seen to be limited by the diaphragm mass.

For subsequent particles, their location and pressure-time history is evaluated analytically using the now known diaphragm trajectory (3) and the straight J_- characteristics.[7] The reflected shock trajectory is computed similarly by evaluating J_- at the diaphragm and communicating it back along the straight characteristics to specify the downstream velocity boundary condition for the shock.

For the holding time model just described, the holding time creates a fully stagnant region. The instantaneous diaphragm rupture that follows forms a centered unsteady expansion anchored to the diaphragm station (Fig. 1c). Shock decay only begins when the head of the expansion intersects the reflected shock. Taking the holding time sufficiently large so that no decay occurs for test gas particles that will comprise the useful test gas, the pressure history for a particle which enters the centered expansion at time t_0 after shock reflection is,[7]

$$\frac{p}{p_0} = \left(\frac{t}{t_0}\right)^{-2\gamma/(\gamma + 1)} \tag{5}$$

where p_0 is the pressure behind the reflected shock and $t \geq t_0$. Different particle histories correspond to different values of t_0. The initial expansion rate at $t = t_0$ is $dp/dt = -2\gamma p_0/(\gamma + 1)t_0$, so that the particle initially adjacent to the diaphragm at rupture, corresponding to $t_0 \to 0$, experiences an infinite expansion rate.

Inertial Diaphragm Model Results

The nominal Mach 17 operating condition[4] of the HYPULSE expansion tube is used for a test case. For this condition the shock tube is filled with air to 3.45 kPa, and the primary shock speed is 2670 m/s approaching the diaphragm. The acceleration tube is filled to 7.2 Pa, also with air, and the diaphragm is 12.7-μm polyester film. Equilibrium conditions behind the reflected shock at the diaphragm are $p_0 = 2.19$ MPa, $a_0 = 1380$ m/s, and $\gamma = 1.30$. The one-dimensional finite volume code of Jacobs[8] was run for this test case using approximate equilibrium chemistry. The solution was started at the time the primary shock reaches the diaphragm and continued for 0.5 ms. The diaphragm was assumed to act as a piston of fixed mass. Grid convergence was confirmed by doubling the resolution and noting no significant change in the solution.

Figure 2a shows a measured tube wall pressure trace[9] at a location 76 mm downstream of the secondary diaphragm with analytical and numerical simulations. The numerical solution accurately predicts the diaphragm location, as well as the initial pressure field. The reflected shock appears to be smeared in the experimental trace, possibly as a result of nonplaner diaphragm rupture. The analytical solution captures the general features of the flowfield, in particular the location and pressure on the diaphragm. In addition, Fig. 2b

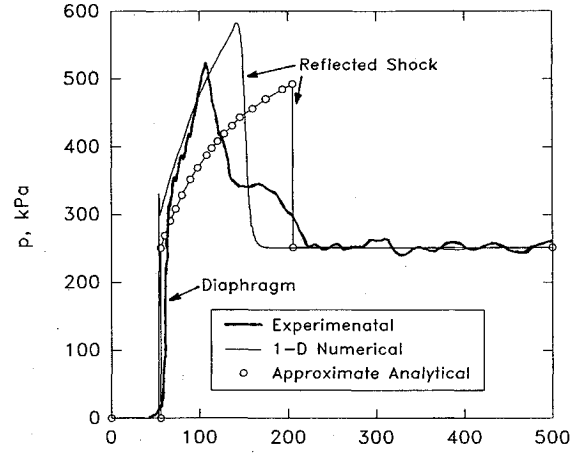

Fig. 2a Pressure history at 76 mm downstream of secondary diaphragm.

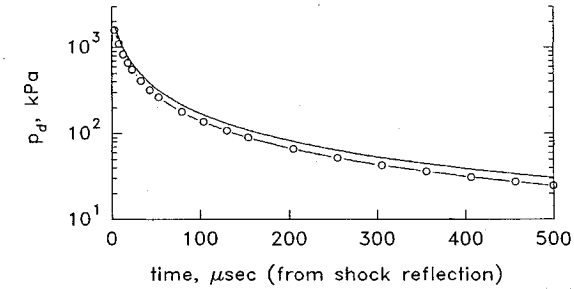

Fig. 2b Calculated pressure on diaphragm upstream surface.

shows that there is good agreement between the numerical and analytical estimates of pressure decay for the particle adjacent to the diaphragm. This also indicates that the effects of chemistry on the pressure distribution are small for the conditions considered and that the ideal gas approximation is adequate for this study.

Recombination Chemistry

Recombination in the expansion is calculated using a general chemical kinetics computer program[10] for a specified particle pressure-time history, with the gas immediately behind the reflected shock assumed to be in chemical equilibrium. There exist several choices for the chemical kinetic rate mechanisms for high-temperature air[11] that give variations of approximately ±20% in the computed atomic oxygen mass fraction. The mechanism in Ref. 12 has been widely used for computing shock tunnel nozzle flows and is adopted here.

Figure 3 shows computed atomic oxygen and nitric oxide mass fractions (the only significant air contaminants at these conditions) as a function of time after flow arrival in the test section located 14 m from the diaphragm at the exit of the acceleration tube. The time ordinate in all cases results from

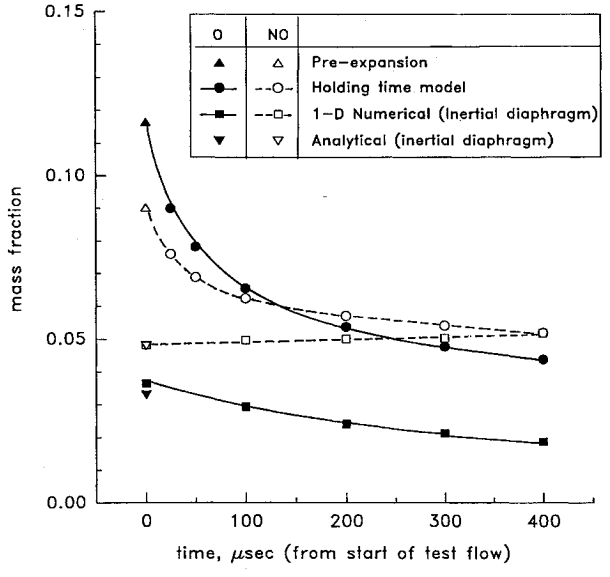

Fig. 3 Atomic oxygen (O) and nitric oxide (NO) mass fractions in the test flow at Mach 17 HYPULSE condition.

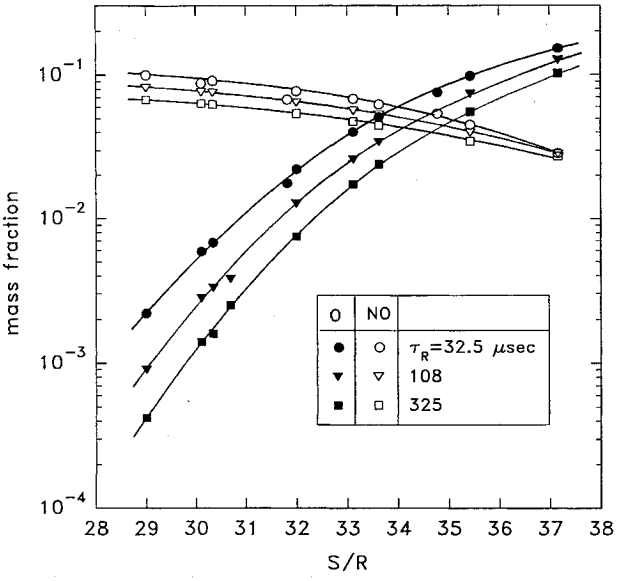

Fig. 4 Entropy-inertia correlation for predicting nonequilibrium air compositions in an expansion tube, $\tau_R = t_R p_0^{(\gamma+1)/2\gamma}$.

conserving mass between a given particle and the diaphragm when going from the postincident shock state, 2, through the reflected shock and expansion, to the facility exit, state 5 (Fig. 1).

Considering the holding time model results, the first particles to exit the facility (those initially adjacent to the diaphragm) experience rapid expansion rates and freeze at a composition near the pre-expansion value. Subsequent particles see lesser expansion rates and recombine further, in agreement with the results of Ref. 5. For the numerical solution of the inertia model, five particle trajectories were analyzed. The presence of the diaphragm mass reduces the expansion rate for the first particles yielding greater recombination than the holding time model. Subsequent particles are processed by a weaker reflected shock altering the composition as shown. Using the pressure history from the analytical solution for the particle adjacent to the diaphragm, good agreement is found with the numerical solution there. Accuracy of the analytical solution diminishes for subsequent particles and they are not analyzed for recombination.

Entropy Correlation

For steady expansion nozzles the frozen enthalpy and composition of nonequilibrium air at the nozzle exit correlate well with the nozzle reservoir entropy.[13,14] Nonequilibrium compositions resulting from unsteady expansion can be similarly correlated using the postreflected shock entropy, provided that the initial portion of the expansion occurs in equilibrium and at constant entropy. For this situation the expansion will pass through the lower pressure starting conditions of other expansions having the same entropy. If these expansions subsequently have coincident pressure-time histories, they will yield the same final composition. From Eq. (4) it can be seen that coincident expansions have equal values of the modified time scale

$$\tau_R = t_R p_0^{(\gamma+1)/2\gamma} \tag{6}$$

All expansions with the same τ_R and initial entropy will yield the same chemical composition.

Figure 4 illustrates this correlation for atomic oxygen and nitric oxide mass fractions. It was constructed for a range of initial pressures of 1.5, 15.0, and 150 MPa and temperatures from 3500 to 6000 K. These ranges should span the majority of expansion tube operating conditions for simulating suborbital velocities. The correlation is accurate to within the uncertainty due to the high-temperature air kinetics already noted. It applies to the particle initially adjacent to the diaphragm, and thus from Fig. 3, represents an upper bound on atomic oxygen and a reasonable estimate of nitric oxide content. Departure from the correlation occurs below 3500 K where the equilibrium starting conditions fall below the freezing condition of expansions from higher pressure and the same entropy. The thermodynamic data available in the kinetics code[10] set the 6000 K maximum temperature limit.

Acknowledgments

This work was supported under a grant from the NASA Langley Research Center, NAGW-674, and by an Australian Overseas Postgraduate Research Scholarship in Australia. The authors also acknowledge R. J. Stalker for instigating the study and P. A. Jacobs for contributing the numerical simulation, both from the University of Queensland, and J. Tamagno from General Applied Science Laboratories for the experimental data.

References

[1]Trimpi, R. L., "A Preliminary Theoretical Study of the Expansion Tube, a New Device for Producing High-Enthalpy Short-Duration Hypersonic Gas Flows," NASA TR-133, 1962.

[2]Shinn, J. L., and Miller, C. G., "Experimental Perfect Gas Study of Expansion-Tube Flow Characteristics," NASA TP 1317, 1978.

[3]Morgan, R. G., and Stalker, R. J., "Double Diaphragm Driven

Free Piston Expansion Tube," *Proceedings 18th International Symposium on Shock Tubes and Waves* (Sendai, Japan, July 1991), Springer-Verlag, 1992.

[4]Tamagno, J., Bakos, R., Pulsonetti, M., and Erdos, J., "Hypervelocity Real Gas Capabilities of GASL's Expansion Tube (HYPULSE) Facility," AIAA Paper 90-1390, June 1990.

[5]Wilson, G. J., "Time-Dependent Quasi-One Dimensional Simulations of High Enthalpy Pulse Facilities," AIAA Paper 92-5096, Dec. 1992.

[6]Meyer, R. F., "The Impact of a Shock Wave on a Movable Wall," *Journal of Fluid Mechanics,* Vol. 3, No. 3, 1957, pp. 309–323.

[7]Courant R., and Friedrichs, K. O., *Supersonic Flow and Shock Waves,* Applied Mathematical Sciences, Vol. 21, Springer-Verlag, New York, 1976, pp. 97–106.

[8]Jacobs, P. A., "Quasi-One-Dimensional Modeling of Free-Piston Shock Tunnels," AIAA Paper 93-0352, Jan. 1993.

[9]Tamagno, J., private communication, General Applied Science Laboratories, Ronkonkoma, NY, July 1992.

[10]Bittker, D. A., and Scullin, V. J., "General Chemical Kinetics Computer Program for Static and Flow Reactions, with Application to Combustion and Shock Tube Kinetics," NASA TN-D-6586, Jan. 1972.

[11]Sagnier, P., and Marraffa, L., "Parametric Study of Thermal and Chemical Nonequilibrium Nozzle Flow," *AIAA Journal,* Vol. 29, No. 3, 1991, pp. 334–343.

[12]Hall, J. G., Eshenroeder, A. Q., and Marrone, P. V., "Blunt-Nose Inviscid Airflows with Coupled Nonequilibrium Processes," *Journal of the Aerospace Sciences,* Vol. 29, No. 9, 1962, pp. 1038–1051.

[13]Lordi, J. A., and Mates, R. E., "Nonequilibrium Effects on High-Enthalpy Expansions of Air," *AIAA Journal,* Vol. 3, No. 10, 1965, pp. 1972–1974.

[14]Harris, C., "Comment on 'Nonequilibrium Effects on High-Enthalpy Expansions of Air'," *AIAA Journal,* Vol. 4, No. 6, 1966, p. 1148.

Sensitivity Derivatives for Three-Dimensional Supersonic Euler Code Using Incremental Iterative Strategy

Vamshi Mohan Korivi,* Arthur C. Taylor III,† and Gene W. Hou‡
Old Dominion University, Norfolk, Virginia 23529
and
Perry A. Newman§ and Henry E. Jones¶
NASA Langley Research Center, Hampton, Virginia 23681

Introduction

In recent work,[1,2] an incremental strategy was proposed to iteratively solve the very large systems of linear equations that are required to obtain quasianalytical sensitivity derivatives from advanced computational fluid dynamics (CFD) codes. The technique was successfully demonstrated for two large two-dimensional problems: a subsonic and a transonic airfoil. The principal feature of this incremental iterative strategy is that it allows the use of the identical approximate coefficient matrix operator and algorithm to solve the nonlinear flow and the linear sensitivity equations; at convergence, the accuracy of the sensitivity derivatives is not compromised. This feature allows a comparatively straightforward extension of the methodology to three-dimensional problems; this extension is successfully demonstrated in the present study for a space-marching solution of the three-dimensional Euler equations over a Mach 2.4 blended wing-body configuration.

Received June 29, 1993; presented in open forum at the AIAA 11th Computational Fluid Dynamics Conference, Orlando, FL, July 6–9, 1993; revision received Nov. 5, 1993; accepted for publication Nov. 6, 1993.

*Graduate Research Assistant, Department of Mechanical Engineering.
†Assistant Professor, Department of Mechanical Engineering. Member AIAA.
‡Associate Professor, Department of Mechanical Engineering. Member AIAA.
§Senior Research Scientist, Computational Science Branch, Fluid Mechanics Division, MS 159.
¶Research Scientist, U.S. Army Aeroflightdynamics Directorate, JRPO, MS 159. Senior Member AIAA.

Theoretical Background

Discretization of the Euler equations and the boundary conditions results in a large system of coupled nonlinear algebraic equations; for a steady-state solution, this system is represented as

$$\boldsymbol{R}[\boldsymbol{Q}(\boldsymbol{D}), \boldsymbol{D}] = 0 \tag{1}$$

where $\boldsymbol{Q}$ is the vector of field variables and $\boldsymbol{D}$ is a vector of input (design) variables. Differentation of Eq. (1) yields the matrix equation

$$\frac{\mathrm{d}\boldsymbol{R}}{\mathrm{d}\boldsymbol{D}} = \frac{\partial \boldsymbol{R}}{\partial \boldsymbol{Q}}\boldsymbol{Q}' + \frac{\partial \boldsymbol{R}}{\partial \boldsymbol{D}} = 0 \tag{2}$$

where $\boldsymbol{Q}' \equiv \mathrm{d}\boldsymbol{Q}/\mathrm{d}\boldsymbol{D}$. The linear Eq. (2) must be solved for $\boldsymbol{Q}'$ for the subsequent computation of the sensitivity derivatives of the aerodynamic output functions $\boldsymbol{F}$ with respect to the input variables $\boldsymbol{D}$:

$$\boldsymbol{F} = \boldsymbol{F}[\boldsymbol{Q}(\boldsymbol{D}), \boldsymbol{D}] \tag{3}$$

Differentiation of Eq. (3) yields

$$\frac{\mathrm{d}\boldsymbol{F}}{\mathrm{d}\boldsymbol{D}} = \frac{\partial \boldsymbol{F}}{\partial \boldsymbol{Q}}\boldsymbol{Q}' + \frac{\partial \boldsymbol{F}}{\partial \boldsymbol{D}} \tag{4}$$

where $\mathrm{d}\boldsymbol{F}/\mathrm{d}\boldsymbol{D}$ are the sensitivity derivatives of interest.

The standard incremental formulation for iteratively solving the nonlinear Eq. (1) is

$$-\frac{\tilde{\partial}\boldsymbol{R}^n}{\partial \boldsymbol{Q}}\Delta\boldsymbol{Q} = \boldsymbol{R}^n$$

$$n = 1, 2, 3, \ldots \tag{1}$$

$$\boldsymbol{Q}^{n+1} = \boldsymbol{Q}^n + \Delta\boldsymbol{Q}$$

With typical CFD methods, the coefficient matrix operator $\tilde{\partial}\boldsymbol{R}^n/\partial\boldsymbol{Q}$ represents only a very rough approximation of the exact Jacobian matrix that would be associated with a strict implementation of Newton-Raphson (NR) iteration. Because of memory limitations, NR iteration is not currently feasible on modern supercomputers (with the use of in-core solvers) for Euler and/or Navier-Stokes codes when applied to large two-dimensional and practical three-dimensional flow problems. This computational difficulty carries over to the linear sensitivity equations, Eq. (2); as a remedy, these equations should be cast into an incremental form and solved iteratively as

$$-\frac{\tilde{\partial}\boldsymbol{R}}{\partial \boldsymbol{Q}}\Delta\boldsymbol{Q}' = \frac{\mathrm{d}\boldsymbol{R}^m}{\mathrm{d}\boldsymbol{D}} = \frac{\partial \boldsymbol{R}}{\partial \boldsymbol{Q}}\boldsymbol{Q}'^m + \frac{\partial \boldsymbol{R}}{\partial \boldsymbol{D}}$$

$$m = 1, 2, 3, \ldots \tag{6}$$

$$\boldsymbol{Q}'^{m+1} = \boldsymbol{Q}'^m + \Delta\boldsymbol{Q}'$$

Comparison of Eqs. (6) with Eqs. (5) reveals that the identical left-hand side, approximate coefficient matrix operator and algorithm can be used to iteratively solve the nonlinear flow equation [Eqs. (1)] and the linear sensitivity equation [Eqs. (2)]. Thus, only a change of the right-hand side is required to solve the sensitivity equations. A more complete discussion of the computational advantages of this procedure is given in Refs. 1 and 2.

Sample Problem

The three-dimensional Euler equations are solved here for a fully supersonic flow with the space-marching method described